

Parameter estimation in a subcritical percolation model with colouring

Felix Beck^{*†}, Bence Mélykúti^{*‡}

25th July 2022

Abstract

In the bond percolation model on a lattice, we colour vertices with n_c colours independently at random according to Bernoulli distributions. A vertex can receive multiple colours and each of these colours is individually observable. The colours colour the entire component into which they fall. Our goal is to estimate the $n_c + 1$ parameters of the model: the probabilities of colouring of single vertices and the probability with which an edge is open. The input data is the configuration of colours once the complete components have been coloured, without the information which vertices were originally coloured or which edges are open.

We use a Monte Carlo method, the method of simulated moments to achieve this goal. We make progress towards proving that this method is a strongly consistent estimator by proving a strong law of large numbers for the vertices' weakly dependent colour values. We evaluate the method in computer tests. The motivating application is cross-contamination rate estimation for digital PCR in lab-on-a-chip microfluidic devices.

Keywords parameter estimation, method of simulated moments, percolation, strong law of large numbers with dependence, microfluidics, cross-contamination

Mathematics subject classification 62F10 (Point estimation), 60K35 (Interacting random processes; statistical mechanics type models; percolation theory)

1 Bond percolation with colouring

We consider bond percolation [14] on the triangular lattice, but our arguments hold for the square lattice as well. Edges are open (that is, included in the graph, alternatively, receive weight 1 as opposed to 0) independently at random with probability $\mu \in [0, 1]$. There are $n_c \in \mathbb{N} \setminus \{0\}$ colours given, and for every colour $\ell \in \{1, 2, \dots, n_c\}$, a parameter $\lambda^\ell \in [0, 1]$ is fixed. For every vertex $i \in I$, the vertex is coloured with colour $\ell \in \{1, 2, \dots, n_c\}$ according to a Bernoulli random variable with probability λ^ℓ . The colouring with different colours is independent in any one vertex, and it is also independent among different vertices. A vertex can receive multiple colours and each of these colours is individually observable. We call this colouring the *seeding*: $X_i^\ell \in \{0, 1\}$ for every $i \in I$ and $\ell \in \{1, 2, \dots, n_c\}$.

These colours propagate through open edges and colour ('contaminate') the entire component they are contained in. Let $i \leftrightarrow j$ mean that vertices $i, j \in I$ are connected by an open path. The

^{*}Centre for Biological Systems Analysis (ZBSA), University of Freiburg, Habsburgerstraße 49, 79104 Freiburg, Germany

[†]Institute for Mathematics, University of Freiburg, Eckerstraße 1, 79104 Freiburg, Germany

[‡]Corresponding author. Email: melykuti@stochastik.uni-freiburg.de.

observed colour configuration is

$$Y_i^\ell := X_i^\ell \vee \bigvee_{j: j \leftrightarrow i} X_j^\ell \in \{0, 1\}$$

for every $i \in I$ and $\ell \in \{1, 2, \dots, n_c\}$, where \vee is the maximum operator.

Our goal is to estimate the parameter $\theta = (\lambda^1, \dots, \lambda^{n_c}, \mu)$ from the data $(Y_i^\ell)_{i \in I, \ell \in \{1, 2, \dots, n_c\}}$ (Figure 1). We assume that I is a finite, connected subset of the lattice and let $n_I := |I|$. (Here connected is meant with all lattice edges considered, not only the open edges.) The spatial arrangement of (Y_i^ℓ) within the lattice is known, but the seeding (X_i^ℓ) and the open or closed state of the edges are unavailable. We bring together three theoretical tools in this paper.

First, parameter estimation is conducted by the *method of simulated moments* (MSM) [12, 13] (Section 2). This is a simulation-based, computationally intensive statistical method that yields a point estimate for θ which converges almost surely to the correct value as $n_I \rightarrow \infty$.

Second, as a first step towards proving the strong consistence of the estimator, we prove a strong law of large numbers (SLLN) with weakly dependent variables. We do this in Section 3 by adapting Theorem 1 of [8].

Third, the SLLN result requires some grasp of how small the dependence is between distant vertices of the lattice. The upper bounds on correlations are provided by the FKG and BK inequalities of percolation theory and the exponential decay of the cluster size distribution [1, 4, 9], [14, Chapters 2 and 6] in Section 4.

Our estimation method is tested on synthetic data with known parameter values in Section 5. In Section 6, the motivating problem is described, and the paper concludes with a discussion of possible improvements in modelling and methodology.

2 Method of simulated moments (MSM)

The MSM is a modification of the classical method of moments for parameter estimation for the case when the moments of the sampling distribution cannot be computed from the parameters in closed form. The MSM proposes to simulate n_s samples of the distribution, repeatedly with different parameter values θ (but with common random variables as θ is changed), and to choose the θ which gives the closest match between moments of the data and that of the simulated data. For its detailed description, we recommend perusing a combination of [13] and [12].

The data $\mathcal{Y} = (\mathcal{Y}_i)_{i \in I}$ originates from a distribution which is parameterised by the unknown $\theta_0 \in \Theta$. θ_0 is called the true value of the parameter. Normally, the \mathcal{Y}_i are independent. A sample from this family of distributions with a general parameter is denoted by $Y = (Y_i)_{i \in I}$. Let K be some n_m -dimensional function of the individual observations Y_i . Let $k(\theta)$ be the expectation of K when K is evaluated on a draw Y_i from the distribution with parameter $\theta \in \Theta$, $k(\theta) := E_\theta[K(Y_i)]$. Thus k is a vector of n_m generalised moments of the distribution of Y_i .

Let g be some multidimensional function that represents estimating constraints. In our case these are distances between observed moments and moments of the model with given parameter value θ :

$$g(\mathcal{Y}_i, \theta) = K(\mathcal{Y}_i) - k(\theta).$$

By introducing E_0 as a shorthand for E_{θ_0} , it is immediate that $E_0[g(\mathcal{Y}_i, \theta_0)] = 0$. However, for the parameter estimation problem to be well posed, we require that

$$E_0[g(\mathcal{Y}_i, \theta)] = 0 \quad \Longleftrightarrow \quad \theta = \theta_0. \tag{1}$$

Implicit in this is that we have at least as many independent equations as parameters.

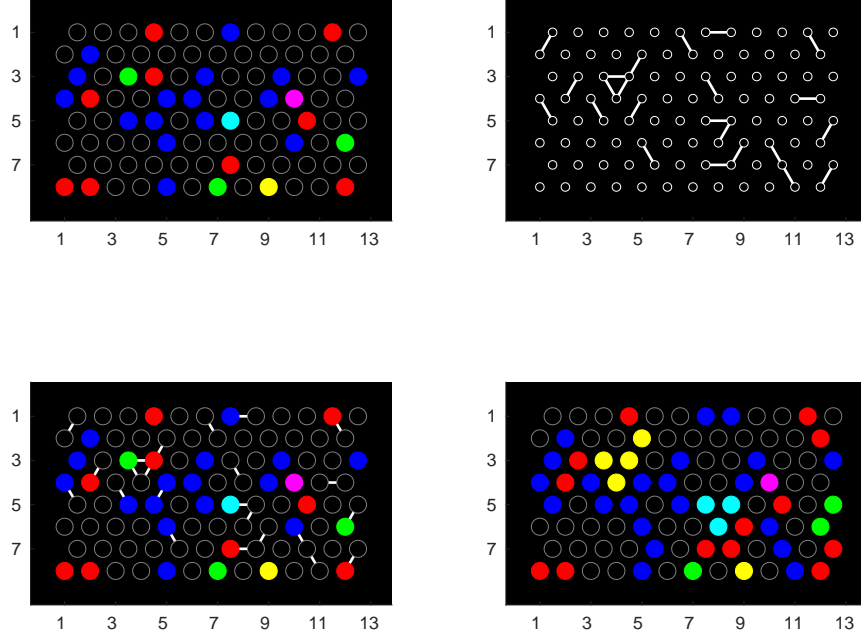


Figure 1: (*top left*) A realisation of random seeding (X_i^ℓ) with $(\lambda^{\text{red}}, \lambda^{\text{green}}, \lambda^{\text{blue}}) = (0.1, 0.05, 0.2)$. (*top right*) A realisation of bond percolation on the triangular lattice with $\mu = 0.1$. (*bottom left*) The bond percolation overlaid with the seeding. (*bottom right*) The resulting configuration (Y_i^ℓ) which serves as the data.

The MSM is used when $k(\theta)$ is not available in analytical form but there exists an unbiased estimator $\tilde{k}(U_i^s, \theta)$, and consequently an unbiased estimator for g , $\tilde{g}(\mathcal{Y}_i, U_i^s, \theta) = K(\mathcal{Y}_i) - \tilde{k}(U_i^s, \theta)$. Here $(U_i^s)_{i \in I, s \in \{1, \dots, n_s\}}$ is some source of randomness, typically vectors of independent, uniform random variables on $[0, 1]$ as provided by a pseudorandom number generator. The estimators satisfy $\mathbb{E}[\tilde{k}(U_i^s, \theta)] = k(\theta)$ and $\mathbb{E}[\tilde{g}(\mathcal{Y}_i, U_i^s, \theta) \mid \mathcal{Y}_i] = g(\mathcal{Y}_i, \theta)$.

We introduce a weighting by a symmetric, positive definite matrix $\Omega \in \mathbb{R}^{n_m \times n_m}$, which might be a function of the data, and consider the quadratic form $\alpha(\eta) = \eta^T \Omega \eta$. The broad principle of the MSM is the following.

Proposition 1 The MSM estimator is defined as

$$\hat{\theta}_{n_s, n_I} := \arg \min_{\theta \in \Theta} \alpha \left(\frac{1}{n_I} \sum_{i=1}^{n_I} \left(K(\mathcal{Y}_i) - \frac{1}{n_s} \sum_{s=1}^{n_s} \tilde{k}(U_i^s, \theta) \right) \right).$$

If identifiability holds, n_s is fixed and n_I tends to infinity, and the almost sure convergence guaranteed by the SLLN

$$\frac{1}{n_I} \sum_{i=1}^{n_I} \tilde{k}(U_i^s, \theta) \xrightarrow[n_I \rightarrow \infty]{} k(\theta) \quad (2)$$

is uniform in $\theta \in \Theta$ for every s , then $\hat{\theta}_{n_s, n_I}$ is strongly consistent (that is, $\hat{\theta}_{n_s, n_I}$ converges to θ_0 almost surely).

Notice that the number of simulations n_s can remain bounded, it is only n_I that must tend to infinity for consistence. For practical implementations, it is a crucial point that the (U_i^s) must be

drawn at the beginning of the exploration of the parameter space and kept fixed afterwards in order to avoid introducing an extra layer of fluctuation [12, p. 29]. This way, a gradient-based search of the parameter space is possible. On the theoretical level, in the limit $n_I \rightarrow \infty$, the estimator is strongly consistent even without using common random numbers.

Under the additional condition that $\tilde{g}(\mathcal{Y}_i, U_i^s, \theta)$ is twice differentiable with respect to θ , asymptotic normality of the estimator also holds and the asymptotic variance can be explicitly given [12, 13].

For the MSM applied to our percolation model with colouring, the data points Y_i are neither identically distributed (because of boundary effects) nor independent, and Proposition 1 does not imply the validity of the method. The main theoretical objective of this research is the proof of the strong consistence of a particular MSM estimator for our estimation problem. However, currently we can prove the SLLN only for any relevant individual parameter vector, but not yet uniformly in $\theta \in \Theta$.

We write $i \sim j$ for adjacent lattice vertices $i, j \in I$ no matter in what state the connecting edge is. The generalised moment function K we propose contains, in addition to first moments Y_i^ℓ , products $Y_i^\ell Y_j^\ell$ for $i \sim j$ because these carry much information about open edges. We note the consequence that it no longer suffices that K is a function of individual Y_i^ℓ only.

We assume without proof that for this generalised moment function identifiability (1) holds. This assumption is not true in some extreme cases which we exclude. If $(\lambda^1, \dots, \lambda^{n_c}) = h \in \{0, 1\}^{n_c}$, then Y is identically h for any choice of μ . The outcome Y is the same with high probability as $n_I \rightarrow \infty$, if $\mu = 1$ and $\lambda^\ell > 0$ if and only if $h_\ell = 1$.

The percolation parameter μ can take any value in the subcritical regime $[0, p_c[$. p_c is the *critical probability* of bond percolation. For the triangular lattice, its value is $p_c = 2 \sin \frac{\pi}{18} \approx 0.3473$, while for the square lattice, it is $p_c = 1/2$ [14, 20, Chapter 3].

Section 3 details the steps leading to the SLLN result (2). Due to dependence between the Y_i , cross-correlations appear in the derivation in addition to variances. Section 4 deals with upper bounding these correlations using percolation theory.

Some further notation will help shorten our formulae. Write $I_2 := \{(i, j) \in I \times I \mid i \sim j, i < j\}$ for the set of ordered pairs of adjacent vertices (independently from whether the connecting edge is open or closed) and $n_p := |I_2|$ for the total number of such neighbouring pairs.

The observed colouring of the dataset is denoted by \mathcal{Y}_i^ℓ ($i \in I$, $\ell \in \{1, 2, \dots, n_c\}$), whereas in the simulated data it is $Y_i^{\ell, s}$ ($s \in \{1, 2, \dots, n_s\}$). Lastly, we introduce the following averages:

$$\begin{aligned} \bar{Y}^\ell &:= \frac{1}{n_I} \sum_{i \in I} \mathcal{Y}_i^\ell, & \bar{Y}^{\ell, s} &:= \frac{1}{n_I} \sum_{i \in I} Y_i^{\ell, s}, \\ \bar{Z}^\ell &:= \frac{1}{n_p} \sum_{(i, j) \in I_2} \mathcal{Y}_i^\ell \mathcal{Y}_j^\ell, & \bar{Z}^{\ell, s} &:= \frac{1}{n_p} \sum_{(i, j) \in I_2} Y_i^{\ell, s} Y_j^{\ell, s}. \end{aligned}$$

Our main claim, currently only conjectured, is the following.

Claim 2 (conjectured) Let Θ be a compact subset of $([0, 1]^{n_c} \setminus \{0, 1\}^{n_c}) \times [0, p_c[$. (For the triangular lattice, $p_c = 2 \sin \frac{\pi}{18} \approx 0.3473$, while in the square lattice case, $p_c = 1/2$.) Consider the bond percolation model with colouring and with the true parameter value $\theta_0 = (\lambda^1, \dots, \lambda^{n_c}, \mu) \in \Theta$. Let $\Omega \in \mathbb{R}^{2n_c \times 2n_c}$ be a symmetric, positive definite matrix, which might be a function of the data, and write $\alpha(\eta) = \eta^T \Omega \eta$ for the resulting quadratic form. Under the assumption of identifiability, when

n_s is fixed and n_I tends to infinity,

$$\begin{aligned}\hat{\theta}_{n_s, n_I} &:= \arg \min_{\theta \in \Theta} \alpha \left(\begin{array}{c} \left(\frac{1}{n_I} \sum_{i \in I} \left(\mathcal{Y}_i^\ell - \frac{1}{n_s} \sum_{s=1}^{n_s} Y_i^{\ell, s} \right) \right)_{\ell \in \{1, \dots, n_c\}} \\ \left(\frac{1}{n_p} \sum_{(i,j) \in I_2} \left(\mathcal{Y}_i^\ell \mathcal{Y}_j^\ell - \frac{1}{n_s} \sum_{s=1}^{n_s} Y_i^{\ell, s} Y_j^{\ell, s} \right) \right)_{\ell \in \{1, \dots, n_c\}} \end{array} \right) \\ &= \arg \min_{\theta \in \Theta} \alpha \left(\begin{array}{c} \left(\bar{\mathcal{Y}}^\ell - \frac{1}{n_s} \sum_{s=1}^{n_s} \bar{Y}^{\ell, s} \right)_{\ell \in \{1, \dots, n_c\}} \\ \left(\bar{\mathcal{Z}}^\ell - \frac{1}{n_s} \sum_{s=1}^{n_s} \bar{Z}^{\ell, s} \right)_{\ell \in \{1, \dots, n_c\}} \end{array} \right)\end{aligned}$$

is strongly consistent.

In order to prove the claim, we want to establish that for the arithmetic means generated under general θ , the following almost sure convergences hold as $n_I \rightarrow \infty$, uniformly in $\theta \in \Theta$:

$$\begin{aligned}\frac{1}{n_I} \sum_{i \in I} Y_i^\ell - \frac{1}{n_I} \sum_{i \in I} \mathbb{E}_\theta Y_i^\ell &\rightarrow 0 \\ \text{and } \frac{1}{n_p} \sum_{(i,j) \in I_2} Y_i^\ell Y_j^\ell - \frac{1}{n_p} \sum_{(i,j) \in I_2} \mathbb{E}_\theta [Y_i^\ell Y_j^\ell] &\rightarrow 0,\end{aligned}$$

for $i \sim j$. This would ensure that

$$\begin{aligned}\alpha \left(\begin{array}{c} \left(\bar{\mathcal{Y}}^\ell - \frac{1}{n_s} \sum_{s=1}^{n_s} \bar{Y}^{\ell, s} \right)_{\ell \in \{1, \dots, n_c\}} \\ \left(\bar{\mathcal{Z}}^\ell - \frac{1}{n_s} \sum_{s=1}^{n_s} \bar{Z}^{\ell, s} \right)_{\ell \in \{1, \dots, n_c\}} \end{array} \right) - \\ \alpha \left(\begin{array}{c} \left(\frac{1}{n_I} \sum_{i \in I} (\mathbb{E}_0 Y_i^\ell - \mathbb{E}_\theta Y_i^\ell) \right)_{\ell \in \{1, \dots, n_c\}} \\ \left(\frac{1}{n_p} \sum_{(i,j) \in I_2} (\mathbb{E}_0 [Y_i^\ell Y_j^\ell] - \mathbb{E}_\theta [Y_i^\ell Y_j^\ell]) \right)_{\ell \in \{1, \dots, n_c\}} \end{array} \right) &\xrightarrow{n_I \rightarrow \infty} 0\end{aligned}$$

uniformly with probability 1. The right term is minimal when it is zero, and this is achieved in only $\theta = \theta_0$ under the assumption of identifiability (1). This gives the strong consistence for $\hat{\theta}_{n_s, n_I}$. This unusual formulation of the strong law of large numbers is needed because the random variables are not identically distributed due to boundary effects. In this paper, we can only prove almost sure convergence for fixed parameter values but not yet uniform convergence.

3 Strong law of large numbers with weak dependence

We adapt the proof of Theorem 1 of [8] in this section to suit our purposes.

Proposition 3 Let Θ be a compact subset of $[0, 1]^{n_c} \times [0, p_c[$, where p_c is the critical probability of bond percolation. If Y is generated with parameter value $\theta \in \Theta$, then

$$\frac{1}{n_I} \left(\sum_{i \in I} Y_i^\ell - \sum_{i \in I} \mathbb{E}_\theta Y_i^\ell \right) \xrightarrow{n_I \rightarrow \infty} 0$$

almost surely.

Proposition 4 Let Θ be a compact subset of $[0, 1]^{n_c} \times [0, p_c[$. If Y is generated with parameter value $\theta \in \Theta$, then

$$\frac{1}{n_p} \left(\sum_{(i,j) \in I_2} Y_i^\ell Y_j^\ell - \sum_{(i,j) \in I_2} \mathbb{E}_\theta [Y_i^\ell Y_j^\ell] \right) \xrightarrow{n_I \rightarrow \infty} 0$$

almost surely.

Proof (Proposition 3) For the ease of notation, let $Y_i := Y_i^\ell$ for some fixed $\ell \in \{1, \dots, n_c\}$ ($i \in I$), created by our percolation process with $\theta = (\lambda^1, \dots, \lambda^{n_c}, \mu)$. Let $a > 1$ and define the lacunary sequence $k_n := \lfloor a^n \rfloor$. Let $S_k := \sum_{i=1}^k Y_i$.

Then by the application of Chebyshov's inequality, for every $\varepsilon > 0$,

$$\begin{aligned} \sum_{n=1}^{\infty} \mathbb{P} \left(\left| \frac{S_{k_n} - \mathbb{E}S_{k_n}}{k_n} \right| > \varepsilon \right) &\leq \sum_{n=1}^{\infty} \frac{\sup_{\theta \in \Theta} \text{Var } S_{k_n}}{\varepsilon^2 k_n^2} \\ &\leq \frac{1}{\varepsilon^2} \sum_{n=1}^{\infty} \frac{1}{k_n^2} \sup_{\theta \in \Theta} \sum_{i=1}^{k_n} \text{Var } Y_i \\ &\quad + \frac{1}{\varepsilon^2} \sum_{n=1}^{\infty} \frac{1}{k_n^2} \sup_{\theta \in \Theta} \sum_{1 \leq i \neq j \leq k_n} (\mathbb{E}[Y_i Y_j] - \mathbb{E}Y_i \mathbb{E}Y_j). \end{aligned} \quad (3)$$

If we can prove that this is finite, then by the Borel–Cantelli lemma, as $n \rightarrow \infty$,

$$\sup_{\theta \in \Theta} \left| \frac{S_{k_n} - \mathbb{E}S_{k_n}}{k_n} \right| \rightarrow 0 \quad \text{a.s.} \quad (4)$$

We first show that

$$\sum_{n=1}^{\infty} \frac{1}{k_n^2} \sup_{\theta \in \Theta} \sum_{i=1}^{k_n} \text{Var } Y_i < \infty$$

by noticing that $\sup_{\theta \in \Theta} \sup_{i \in I} \text{Var } Y_i \leq 1$ and by the following lemma.

Lemma 5 If $1 < a$, then

$$\sum_{n=1}^{\infty} \frac{1}{k_n} < \infty.$$

Proof For $n \in \mathbb{N}$ sufficiently large, $a^n/2 \leq k_n$ because $n \geq \frac{\log 2}{\log a}$ suffices. To see this, consider that $a^n/2 \leq a^n - 1 < k_n$ is achieved, giving the threshold, if $2 \leq a^n$. Let

$$N_0 := \max \left\{ 1, \left\lceil \frac{\log 2}{\log a} \right\rceil \right\}.$$

Consequently, for some constant c ,

$$\sum_{n=1}^{\infty} \frac{1}{k_n} = \sum_{n=1}^{N_0-1} \frac{1}{k_n} + \sum_{n=N_0}^{\infty} \frac{1}{k_n} \leq c + \sum_{n=N_0}^{\infty} \frac{2}{a^n} = c + \frac{2}{a^{N_0}(1-1/a)} < \infty. \quad \square$$

We will prove in Section 4 that

$$\sup_{\theta \in \Theta} \left| \sum_{1 \leq i \neq j \leq k_n} (\mathbb{E}[Y_i Y_j] - \mathbb{E}Y_i \mathbb{E}Y_j) \right| = \mathcal{O}(k_n), \quad (5)$$

so that by applying Lemma 5 once again, we get that (3) is finite, as required.

In the case of a general $k := n_I$, k is sandwiched between some $k_n \leq k < k_{n+1}$ and

$$\frac{S_k - \mathbb{E}S_k}{k} \leq \left| \frac{S_{k_{n+1}} - \mathbb{E}S_{k_{n+1}}}{k_{n+1}} \right| \frac{k_{n+1}}{k_n} + \frac{\mathbb{E}S_{k_{n+1}} - \mathbb{E}S_{k_n}}{k_n}.$$

Here, for a fixed $a > 1$,

$$\frac{k_{n+1}}{k_n} = \frac{\lfloor a^{n+1} \rfloor}{\lfloor a^n \rfloor} \leq \frac{a^{n+1}}{a^n - 1} = a + \frac{a}{a^n - 1}, \quad (6)$$

which in turn is arbitrarily close to a when n is sufficiently large. Additionally,

$$\begin{aligned} \sup_{\theta \in \Theta} \frac{\mathbb{E}S_{k_{n+1}} - \mathbb{E}S_{k_n}}{k_n} &\leq \frac{(k_{n+1} - k_n) \sup_{\theta \in \Theta} \sup_{i \in I} \mathbb{E}Y_i}{k_n} \\ &\leq \left(a + \frac{a}{a^n - 1} - 1 \right) \sup_{\theta \in \Theta} \sup_{i \in I} \mathbb{E}Y_i, \end{aligned}$$

and combining this with (4) yields

$$\limsup_{k \rightarrow \infty} \sup_{\theta \in \Theta} \frac{S_k - \mathbb{E}S_k}{k} \leq (a-1) \sup_{\theta \in \Theta} \sup_{i \in I} \mathbb{E}Y_i \leq a-1.$$

A similar lower bound can also be attained. Since $a > 1$ can be chosen arbitrarily, the strong law of large numbers for Y_i (Proposition 3) holds once we prove the estimate (5). \square

Proof (Proposition 4) This proof goes entirely analogously to that of Proposition 3. First, let us fix an ordering of the vertices of the infinite triangular lattice such that as $n_I \rightarrow \infty$, I has the property that $n_p \sim 3n_I$ (asymptotic equality). This expresses that I does not have an excessively large or complicated boundary and that boundary effects can be ignored; informally, I as a subset of the lattice should be about as wide as tall, without holes in it.

We keep using the notation $Y_i := Y_i^\ell$ for some fixed $\ell \in \{1, \dots, n_c\}$ and the lacunary sequence $k_n = \lfloor a^n \rfloor$ for $a > 1$. Let $T_k := \sum_{(i,j) \in I_2} Y_i Y_j$ for $I = I(k)$ composed of the first k vertices according to the fixed ordering. This sum has $n_p(k)$ terms. Then, by the argument of (3), for every $\varepsilon > 0$,

$$\begin{aligned} \sum_{n=1}^{\infty} \mathbb{P} \left(\left| \frac{T_{k_n} - \mathbb{E}T_{k_n}}{n_p(k_n)} \right| > \varepsilon \right) &\leq \sum_{n=1}^{\infty} \frac{\sup_{\theta \in \Theta} \text{Var } T_{k_n}}{\varepsilon^2 n_p(k_n)^2} \\ &\leq \frac{1}{\varepsilon^2} \sum_{n=1}^{\infty} \frac{1}{n_p(k_n)^2} \sup_{\theta \in \Theta} \sum_{(i_1, i_2) \in I_2(k_n)} \text{Var } Y_{i_1} Y_{i_2} \\ &\quad + \frac{1}{\varepsilon^2} \sum_{n=1}^{\infty} \frac{1}{n_p(k_n)^2} \sup_{\theta \in \Theta} \sum_{\substack{(i_1, i_2), (j_1, j_2) \in I_2(k_n) \\ (i_1, i_2) \neq (j_1, j_2)}} \left(\mathbb{E}[Y_{i_1} Y_{i_2} Y_{j_1} Y_{j_2}] \right. \\ &\quad \left. - \mathbb{E}[Y_{i_1} Y_{i_2}] \mathbb{E}[Y_{j_1} Y_{j_2}] \right). \end{aligned} \quad (7)$$

By

$$\sup_{\theta \in \Theta} \sup_{(i_1, i_2) \in I_2(k_n)} \text{Var } Y_{i_1} Y_{i_2} \leq 1$$

and $|I_2(k_n)| = n_p(k_n) \sim 3n_I = 3k_n$, Lemma 5 gives

$$\frac{1}{\varepsilon^2} \sum_{n=1}^{\infty} \frac{1}{n_p(k_n)^2} \sup_{\theta \in \Theta} \sum_{(i_1, i_2) \in I_2(k_n)} \text{Var } Y_{i_1} Y_{i_2} \leq \frac{1}{\varepsilon^2} \sum_{n=1}^{\infty} \frac{1}{n_p(k_n)} < \infty.$$

In Section 4, it will be shown that

$$\sup_{\theta \in \Theta} \left| \sum_{\substack{(i_1, i_2), (j_1, j_2) \in I_2(k_n) \\ (i_1, i_2) \neq (j_1, j_2)}} \left(\mathbb{E}[Y_{i_1} Y_{i_2} Y_{j_1} Y_{j_2}] - \mathbb{E}[Y_{i_1} Y_{i_2}] \mathbb{E}[Y_{j_1} Y_{j_2}] \right) \right| = \mathcal{O}(k_n), \quad (8)$$

and by Lemma 5, we get that the sum (7) is finite. By the Borel–Cantelli lemma,

$$\sup_{\theta \in \Theta} \left| \frac{T_{k_n} - \mathbb{E}T_{k_n}}{n_p(k_n)} \right| \rightarrow 0 \quad \text{a.s.} \quad (9)$$

For a general $k = n_I$ with $k_n \leq k < k_{n+1}$,

$$\frac{T_k - \mathbb{E}T_k}{n_p(k)} \leq \left| \frac{T_{k_{n+1}} - \mathbb{E}T_{k_{n+1}}}{n_p(k_{n+1})} \right| \frac{n_p(k_{n+1})}{n_p(k)} + \frac{\mathbb{E}T_{k_{n+1}} - \mathbb{E}T_{k_n}}{n_p(k_n)}. \quad (10)$$

For a fixed $a > 1$, by using (6) again,

$$\frac{n_p(k_{n+1})}{n_p(k_n)} \sim \frac{3k_{n+1}}{3k_n} \leq a + \frac{a}{a^n - 1},$$

and the right-hand side is arbitrarily close to a when n is sufficiently large. Additionally,

$$\sup_{\theta \in \Theta} \frac{ET_{k_{n+1}} - ET_{k_n}}{n_p(k_n)} \leq \frac{(n_p(k_{n+1}) - n_p(k_n)) \sup_{\theta \in \Theta} \sup_{(i_1, i_2) \in I_2(k_n)} E[Y_{i_1} Y_{i_2}]}{n_p(k_n)},$$

hence

$$\limsup_{n \rightarrow \infty} \sup_{\theta \in \Theta} \frac{ET_{k_{n+1}} - ET_{k_n}}{n_p(k_n)} \leq (a - 1) \sup_{\theta \in \Theta} \sup_{(i_1, i_2) \in I_2(k_n)} E[Y_{i_1} Y_{i_2}].$$

Combining this with (9) and (10), we get

$$\limsup_{k \rightarrow \infty} \sup_{\theta \in \Theta} \frac{T_k - ET_k}{n_p(k)} \leq (a - 1) \sup_{\theta \in \Theta} \sup_{(i_1, i_2) \in I_2(k_n)} E[Y_{i_1} Y_{i_2}] \leq a - 1.$$

A similar lower bound can also be attained. Since $a > 1$ can be chosen arbitrarily, the strong law of large numbers for $Y_i Y_j$, $i \sim j$ (Proposition 4) holds once we prove the estimate (8). \square

4 Upper bound on correlations

We prove the estimates (5) and (8) in greater generality, for every positive integer n . Recall that Θ is defined with μ smaller than the percolation threshold.

Lemma 6 As $n \rightarrow \infty$, it holds

$$\sup_{\theta \in \Theta} \left| \sum_{1 \leq i \neq j \leq n} (E[Y_i Y_j] - EY_i EY_j) \right| = \mathcal{O}(n).$$

Lemma 7 As $n \rightarrow \infty$, it holds

$$\sup_{\theta \in \Theta} \left| \sum_{\substack{(i_1, i_2), (j_1, j_2) \in I_2(n) \\ (i_1, i_2) \neq (j_1, j_2)}} \left(E[Y_{i_1} Y_{i_2} Y_{j_1} Y_{j_2}] - E[Y_{i_1} Y_{i_2}] E[Y_{j_1} Y_{j_2}] \right) \right| = \mathcal{O}(n).$$

For background, first we recapitulate from the fundamentals of percolation theory the meaning of increasing events, the FKG inequality, disjoint occurrence and the BK inequality [14, Chapter 2]. It is well known that these concepts do not rely on the specific structure of the lattice graph and can be cast more generally in terms of functions of Boolean variables.

In this vein, one can consider a probability space (Γ, \mathcal{F}, P) with sample space $\Gamma = \{0, 1\}^S$ (S is finite or at most countably infinite) where the set of events \mathcal{F} is the σ -algebra generated by the finite-dimensional cylinder sets and the measure is a product measure

$$P = \prod_{s \in S} \nu_s$$

where ν_s is specified by some vector $(p(s))_{s \in S} \in [0, 1]^S$ via

$$\nu_s(\omega(s) = 1) = p(s), \quad \nu_s(\omega(s) = 0) = 1 - p(s)$$

for sample vectors $(\omega(s))_{s \in S} \in \{0, 1\}^S$ [14, Chapter 2, p33].

In our application, we have already fixed a colour $\ell \in \{1, \dots, n_c\}$ and look at colours independently. We extend the set of edges of the triangular lattice with a loop edge at each vertex, and the value assigned to this loop edge indicates the presence or absence of seeding. For the loop edges, $p(s) = \lambda^\ell$, and for the edges of the lattice which represent contamination, $p(s) = \mu$.

An event $A \in \mathcal{F}$ of the σ -algebra is called *increasing*, if whenever $\omega \leq \omega'$, $\omega \in A$ implies $\omega' \in A$.

Theorem 8 (FKG inequality [9],[14, pp. 34–36]) If A and B are increasing events in \mathcal{F} , then $P(A \cap B) \geq P(A)P(B)$.

Let e_1, e_2, \dots, e_N be N distinct edges of the graph, and $A, B \in \mathcal{F}$ two increasing events which depend on the vector of the states of these N edges $\omega = (\omega(e_1), \dots, \omega(e_N))$ only. Such vectors ω are characterised uniquely by the set of edges with value 1: $J(\omega) = \{e_i \mid i \in \{1, \dots, N\}, \omega(e_i) = 1\}$.

For the increasing events A, B , the event $A \circ B$ (we say A and B occur disjointly) is the set of all $\omega \in \Gamma$ for which there exists an $H \subseteq J(\omega)$ such that ω' determined by $J(\omega') = H$ belongs to A , and ω'' determined by $J(\omega'') = J(\omega) \setminus H$ belongs to B . In words, $A \circ B$ is the set of assignments of 0 and 1 to the edges for which there exist two disjoint sets of edges assigned the value 1 (*open edges*) such that the first such set ensures the occurrence of event A and the second set ensures the occurrence of B . It is easy to verify that $A \circ B$ is also increasing and $A \circ B \subseteq A \cap B$.

The classical example for disjoint occurrence is when A is the event that there is an open path joining i_1 to j_1 within the finite subgraph given by $\{e_1, \dots, e_N\}$ and B is the event that there is an open path between i_2 and j_2 within the same finite subgraph. Then $A \circ B$ is the event that there exist two edge-disjoint paths, the first between i_1 and j_1 and another one joining i_2 to j_2 .

Theorem 9 (BK inequality [4],[14, pp. 37–41]) If A and B are increasing events in \mathcal{F} , then $P(A \circ B) \leq P(A)P(B)$.

Proof (Lemma 6) In the extended lattice graph that has loop edges with weight zero or one at every vertex for seeding, the event $\{Y_i = 1\}$ for $i \in I$ is increasing because it is increasing in both seeding and contamination edges. For any $i, j \in I$,

$$E[Y_i Y_j] - EY_i EY_j = P(Y_i Y_j = 1) - P(Y_i = 1)P(Y_j = 1) \geq 0$$

by the FKG inequality. Hence, for every $\theta \in \Theta$,

$$\sum_{1 \leq i \neq j \leq n} (E[Y_i Y_j] - EY_i EY_j) \geq 0.$$

For the upper bound, consider that

$$\begin{aligned} P(Y_i Y_j = 1) - P(Y_i = 1)P(Y_j = 1) &= P(\{Y_i = 1\} \circ \{Y_j = 1\}) - P(Y_i = 1)P(Y_j = 1) \\ &\quad + P(\{Y_i Y_j = 1\} \setminus \{Y_i = 1\} \circ \{Y_j = 1\}) \\ &\leq P(\{Y_i Y_j = 1\} \setminus \{Y_i = 1\} \circ \{Y_j = 1\}) \end{aligned} \quad (11)$$

by the BK inequality. Cooccurrence of $\{Y_i = 1\}$ and $\{Y_j = 1\}$ which is not disjoint is one where i and j are in the same component:

$$\{Y_i Y_j = 1\} \setminus \{Y_i = 1\} \circ \{Y_j = 1\} \subseteq \{i \leftrightarrow j\}.$$

We show that

$$\sum_{1 \leq i \neq j \leq n} P(i \leftrightarrow j) = \mathcal{O}(n) \quad (12)$$

for $\mu < p_c$, and uniformly so for $\mu \in [0, p_c - \varepsilon]$ for every $\varepsilon > 0$. It follows from the exponential decay of the cluster size distribution and it will complete the proof of Lemma 6.

Let $C(i)$ denote the set of vertices in the component of $i \in I$. Then, writing the probability as the expectation of an indicator function,

$$\sum_{1 \leq i \neq j \leq n} P(i \leftrightarrow j) = \sum_{1 \leq i \leq n} \sum_{\substack{1 \leq j \leq n \\ j \neq i}} E\chi_{\{i \leftrightarrow j\}} = \sum_{1 \leq i \leq n} E[|C(i)| - 1].$$

Theorem 10 (Exponential decay of the cluster size distribution [1], [14, Chapter 6]) For $\mu \in]0, p_c[$, there exists $f(\mu) > 0$ such that for all $k \geq 1$ and $i \in I$, for the bond percolation with parameter μ , it holds that $P(|C(i)| \geq k) \leq e^{-kf(\mu)}$.

Take $\mu' = p_c - \varepsilon$. As $P(|C(i)| \geq k)$ is nondecreasing in μ , we get a uniform bound in $\theta \in \Theta$ if the bound is valid for μ' :

$$\begin{aligned} \sum_{i=1}^n E[|C(i)| - 1] &= \sum_{i=1}^n \left(\left(\sum_{k=1}^{\infty} P(|C(i)| \geq k) \right) - 1 \right) \\ &\leq \sum_{i=1}^n \sum_{k=1}^{\infty} e^{-kf(\mu')} = n \frac{1}{e^{f(\mu')} - 1}. \end{aligned} \quad (13)$$

Proof (Lemma 7) The proof follows closely that of Lemma 6. For any two pairs $(i_1, i_2), (j_1, j_2) \in I_2$,

$$E[Y_{i_1} Y_{i_2} Y_{j_1} Y_{j_2}] - E[Y_{i_1} Y_{i_2}] E[Y_{j_1} Y_{j_2}] \geq 0$$

due to the FKG inequality applied to $\{Y_{i_1} Y_{i_2} = 1\}$ and $\{Y_{j_1} Y_{j_2} = 1\}$. Therefore, for any $\theta \in \Theta$,

$$\sum_{\substack{(i_1, i_2), (j_1, j_2) \in I_2(n) \\ (i_1, i_2) \neq (j_1, j_2)}} \left(E[Y_{i_1} Y_{i_2} Y_{j_1} Y_{j_2}] - E[Y_{i_1} Y_{i_2}] E[Y_{j_1} Y_{j_2}] \right) \geq 0.$$

The first step towards the upper bound, similarly to (11), uses the BK inequality:

$$\begin{aligned} P(Y_{i_1} Y_{i_2} Y_{j_1} Y_{j_2} = 1) - P(Y_{i_1} Y_{i_2} = 1) P(Y_{j_1} Y_{j_2} = 1) \\ \leq P(\{Y_{i_1} Y_{i_2} Y_{j_1} Y_{j_2} = 1\} \setminus \{Y_{i_1} Y_{i_2} = 1\} \circ \{Y_{j_1} Y_{j_2} = 1\}). \end{aligned}$$

Cooccurrence which is not disjoint is one where at least one of i_1 and i_2 is connected to at least one of j_1 and j_2 , or in symbols,

$$\{Y_{i_1} Y_{i_2} Y_{j_1} Y_{j_2} = 1\} \setminus \{Y_{i_1} Y_{i_2} = 1\} \circ \{Y_{j_1} Y_{j_2} = 1\} \subseteq \{i_1 \leftrightarrow \{j_1, j_2\}\} \cup \{i_2 \leftrightarrow \{j_1, j_2\}\},$$

where \leftrightarrow is meant to be reflective so that not disjoint cooccurrence might involve e.g. that $i_1 = j_1$. So for every fixed $\theta \in \Theta$,

$$\begin{aligned} \sum_{\substack{(i_1, i_2), (j_1, j_2) \in I_2(n) \\ (i_1, i_2) \neq (j_1, j_2)}} \left(E[Y_{i_1} Y_{i_2} Y_{j_1} Y_{j_2}] - E[Y_{i_1} Y_{i_2}] E[Y_{j_1} Y_{j_2}] \right) \\ \leq \sum_{\substack{(i_1, i_2), (j_1, j_2) \in I_2(n) \\ (i_1, i_2) \neq (j_1, j_2)}} \left(P(i_1 \leftrightarrow \{j_1, j_2\}) + P(i_2 \leftrightarrow \{j_1, j_2\}) \right). \end{aligned}$$

It suffices to treat the two terms individually, and one of them gives

$$\begin{aligned}
\sum_{\substack{(i_1, i_2), (j_1, j_2) \in I_2(n) \\ (i_1, i_2) \neq (j_1, j_2)}} P(i_1 \leftrightarrow \{j_1, j_2\}) &\leq \sum_{i_1 \in I(n)} \sum_{i_2 \sim i_1} \sum_{(j_1, j_2) \in I_2(n) \setminus \{(i_1, i_2)\}} \left(P(i_1 \leftrightarrow j_1) + P(i_1 \leftrightarrow j_2) \right) \\
&\leq \sum_{i_1 \in I(n)} \sum_{i_2 \sim i_1} \left(\sum_{\substack{(j_1, j_2) \in I_2(n) \setminus \{(i_1, i_2)\} \\ j_1 = i_1}} 2 + \sum_{\substack{(j_1, j_2) \in I_2(n) \setminus \{(i_1, i_2)\} \\ j_2 = i_1}} 2 \right. \\
&\quad \left. + \sum_{(j_1, j_2) \in (I(n) \setminus \{i_1\})_2} \left(P(i_1 \leftrightarrow j_1) + P(i_1 \leftrightarrow j_2) \right) \right) \\
&\leq 6 \times 2 \sum_{i_1 \in I(n)} \left(5 \times 2 + 6 \sum_{j_1 \in I(n) \setminus \{i_1\}} P(i_1 \leftrightarrow j_1) \right) \\
&\leq 12n \left(10 + 6 \frac{1}{e^{f(\mu')} - 1} \right) = \mathcal{O}(n),
\end{aligned}$$

where in the second inequality, we separate between cases when $i_1 = j_1$ or $i_1 = j_2$ and when not, and notice that when they are not equal, then all (j_1, j_2) pairs are disjoint from i_1 . In the third inequality, we replace the sum for $i_2 \sim i_1$ by a factor of 6 (for the triangular lattice), and instead of (j_1, j_2) , we sweep for j_1 , and then for its at most 6 neighbours j_2 separately. Thereby we reduced the problem to the previous case and the fourth inequality follows by (13). This proves Lemma 7, which in turn partially proves Claim 2. \square

5 Computer testing of the proposed method

5.1 Implementation

We implemented the proposed MSM parameter estimator in the MATLAB software (The MathWorks, Inc.) for $n_c = 3$ colours [3], and we report our findings in this section. For the the objective function

$$\alpha \left(\begin{pmatrix} \bar{\mathcal{Y}}^\ell - \frac{1}{n_s} \sum_{s=1}^{n_s} \bar{Y}^{\ell, s} \\ \bar{\mathcal{Z}}^\ell - \frac{1}{n_s} \sum_{s=1}^{n_s} \bar{Z}^{\ell, s} \end{pmatrix}_{\ell \in \{1, \dots, n_c\}} \right), \quad (14)$$

we chose the quadratic form $\alpha(\eta) = \eta^T \Omega \eta$ the following way:

$$\Omega = \text{diag} \left((\bar{\mathcal{Y}}^1)^{-2}, \dots, (\bar{\mathcal{Y}}^{n_c})^{-2}, (\bar{\mathcal{Z}}^1)^{-2}, \dots, (\bar{\mathcal{Z}}^{n_c})^{-2} \right).$$

In the unlikely case that a $\bar{\mathcal{Y}}^\ell$ or a $\bar{\mathcal{Z}}^\ell$ is zero, the corresponding diagonal element of Ω is set to 1. Through this normalisation, we expect each coordinate to contribute roughly equally to the sum.

Common random numbers are used during the exploration of the parameter space. This removes an element of fluctuation as different $\theta = (\lambda^1, \dots, \lambda^{n_c}, \mu) \in \Theta$ are tested. We propose two alternative methods for sampling synthetic datasets. Method 1 is the canonical approach. We draw and fix independent random variables from the uniform distribution on $[0, 1]$: $(U_i^{\ell, s})$ for $\ell \in \{1, \dots, n_c\}$, $s \in \{1, \dots, n_s\}$, $i \in I$, and (V_{ij}^s) for $s \in \{1, \dots, n_s\}$, $(i, j) \in I_2$. Thereafter, for each parameter vector, seeding and the open or closed state of edges are defined by

$$\begin{aligned}
X_i^{\ell, s} &:= \begin{cases} 1 & \text{if } U_i^{\ell, s} < \lambda^\ell, \\ 0 & \text{otherwise,} \end{cases} & \text{for } \ell \in \{1, \dots, n_c\}, s \in \{1, \dots, n_s\}, i \in I; \\
\xi_{ij}^s &:= \begin{cases} 1 & \text{if } V_{ij}^s < \mu, \\ 0 & \text{otherwise,} \end{cases} & \text{for } s \in \{1, \dots, n_s\}, (i, j) \in I_2.
\end{aligned}$$

This method gives a binomially distributed number of open edges and, similarly, seeded vertices for each colour ℓ .

We anticipate that it is beneficial for the parameter estimation to remove the randomness in the numbers of seeds and open edges, and to make exactly as many edges open as their expected number, $\zeta(\mu n_p)$, where ζ is the rounding to the nearest integer with some tie-breaking rule. The same is stipulated for seeds: $\zeta(\lambda^\ell n_I)$ random vertices shall be seeded with colour ℓ . This is what Method 2 does. We see this as a variance-reduction trick that achieves lower variance by introducing dependencies between random draws: for example, by knowing the state of all edges but one, we can infer the state of the remaining edge.

Let S_n denote the set of permutations of $\{1, \dots, n\}$. In Method 2, one draws permutations $(\sigma^{\ell,s})$ from S_{n_I} independently, uniformly at random for $\ell \in \{1, \dots, n_c\}$, $s \in \{1, \dots, n_s\}$, and independent permutations (τ^s) from S_{n_p} uniformly at random for $s \in \{1, \dots, n_s\}$. With these permutations fixed, for each $\theta \in \Theta$, one lets

$$X_i^{\ell,s} := \begin{cases} 1 & \text{if } \sigma^{\ell,s}(i) \leq \zeta(\lambda^\ell n_I), \\ 0 & \text{otherwise,} \end{cases} \quad \text{for } \ell \in \{1, \dots, n_c\}, s \in \{1, \dots, n_s\}, i \in I;$$

$$\xi_{ij}^s := \begin{cases} 1 & \text{if } \tau^s((i,j)) \leq \zeta(\mu n_p), \\ 0 & \text{otherwise,} \end{cases} \quad \text{for } s \in \{1, \dots, n_s\}, (i,j) \in I_2.$$

Minimisation over the parameter space Θ is conducted with the MATLAB routine `fminsearchbnd` [7] for constrained optimisation. $\lambda_{\max}^\ell := \bar{\mathcal{Y}}^\ell$ is certainly an upper bound on what λ^ℓ any point estimator might estimate ($\ell \in \{1, \dots, n_c\}$) as this is the moment estimate in case $\mu = 0$. The upper bound μ_{\max} on μ is left to the user's judgement.

The third and last user input in addition to n_s and μ_{\max} is n_{opt} which specifies how many different initial states to try for the optimisation runs. We expect an inverse relationship between seeding rates and the contamination rate, given the data. Thus the initial parameter values for $k \in \{1, \dots, n_{\text{opt}}\}$ are chosen as

$$\lambda_{\text{initial}}^\ell(k) = \left(1 - \frac{k-1}{n_{\text{opt}}}\right) \lambda_{\max}^\ell, \quad \text{for } \ell \in \{1, \dots, n_c\},$$

$$\mu_{\text{initial}}(k) = 0 + \chi_{\{n_{\text{opt}} > 1\}} \frac{k-1}{n_{\text{opt}}-1} \mu_{\max}.$$

5.2 Results

In order to test the performance of the proposed estimation procedure, we created a number of synthetic datasets with $n_c = 3$ colours, different sizes and different, known parameter vectors using Method 1. Tables 1–4 report the results of estimating $\theta_0 = (\lambda^1, \lambda^2, \lambda^3, \mu)$ using different input settings $(n_s, n_{\text{opt}}, \mu_{\max})$.

The two estimators are denoted by $\hat{\theta}_{n_s, n_I}^{(\text{M1})}$ and $\hat{\theta}_{n_s, n_I}^{(\text{M2})}$ for Methods 1 and 2 of random number generation, respectively. We display the relative bias of the estimators in percentage terms:

$$d^{(\text{M1})} = 100 \left| 1 - \hat{\theta}_{n_s, n_I}^{(\text{M1})} / \theta_0 \right|$$

(the operations are coordinatewise), and analogously, $d^{(\text{M2})}$ for $\hat{\theta}_{n_s, n_I}^{(\text{M2})}$. Finally, we let $\alpha_{\hat{\theta}_{n_s, n_I}^{(\text{M2})}}$ denote the value of the objective function α in (14) at $\hat{\theta}_{n_s, n_I}^{(\text{M2})}$.

We found no definitive answer as to whether Method 1 or 2 is preferable, but the larger n_I values support the superiority of Method 2 (especially the second estimate in Table 3 and Table 4).

Broadly, the relative bias of the estimates become smaller as n_I grows. From $n_I = 25 \times 25 = 625$ to $n_I = 500 \times 500 = 250000$, the relative bias of the estimation of μ improves from about 33%

n_s	n_{opt}	μ_{max}	θ_0	$\hat{\theta}_{n_s, n_I}^{(\text{M1})}$	$d^{(\text{M1})}$	$\hat{\theta}_{n_s, n_I}^{(\text{M2})}$	$d^{(\text{M2})}$	$\alpha_{\hat{\theta}_{n_s, n_I}^{(\text{M2})}}$
10	10	0.1	0.1	0.1287	28.7%	0.1223	22.3%	0.0126
			0.05	0.0597	19.4%	0.0605	21%	
			0.07	0.0614	12.29%	0.0587	16.14%	
			0.06	0.0428	28.67%	0.0436	27.33%	
50	10	0.1	0.1	0.1248	24.8%	0.1229	22.9%	0.0107
			0.05	0.0627	25.4%	0.0626	25.2%	
			0.07	0.0595	15%	0.0602	14%	
			0.06	0.0420	30%	0.0403	32.83%	
100	10	0.1	0.1	0.1339	33.9%	0.1271	27.1%	0.0062
			0.05	0.0629	25.8%	0.0592	18.4%	
			0.07	0.0607	13.29%	0.0606	13.43%	
			0.06	0.0396	34%	0.0413	31.17%	

Table 1: Three estimates for a synthetic dataset with $n_I = 25 \times 25 = 625$ vertices ($n_p = 1776$) and $\theta_0 = (0.1, 0.05, 0.07, 0.06)$.

n_s	n_{opt}	μ_{max}	θ_0	$\hat{\theta}_{n_s, n_I}^{(\text{M1})}$	$d^{(\text{M1})}$	$\hat{\theta}_{n_s, n_I}^{(\text{M2})}$	$d^{(\text{M2})}$	$\alpha_{\hat{\theta}_{n_s, n_I}^{(\text{M2})}}$
20	10	0.05	0.07	0.0734	4.86%	0.0728	4%	0.00020
			0.05	0.0508	1.6%	0.0497	0.6%	
			0.04	0.0390	2.5%	0.0393	1.75%	
			0.03	0.0259	13.67%	0.0258	14%	
40	10	0.05	0.07	0.0736	5.14%	0.0738	5.43%	0.00014
			0.05	0.0504	0.8%	0.0497	0.6%	
			0.04	0.0392	2%	0.0391	2.25%	
			0.03	0.0254	15.33%	0.0256	14.67%	

Table 2: Two estimates for a synthetic dataset with $n_I = 100 \times 100 = 10000$ vertices ($n_p = 29601$) and $\theta_0 = (0.07, 0.05, 0.04, 0.03)$.

to below 5%. In the smallest dataset, Table 1, one can observe that λ^1 and λ^2 are consistently overestimated, whereas λ^3 and μ are underestimated in all six estimations. This turned out to be due to a quirk of the randomly generated dataset. While $(\lambda^1, \lambda^2, \lambda^3) = (0.1, 0.05, 0.07)$, in reality, the dataset had

$$\frac{1}{n_I} \left(\sum_{i \in I} \mathcal{X}_i^1, \sum_{i \in I} \mathcal{X}_i^2, \sum_{i \in I} \mathcal{X}_i^3 \right) = (0.1072, 0.0528, 0.0640).$$

One can notice that in Table 1, λ^1 and λ^2 are overestimated to a greater extent than how much λ^3 is underestimated. Then the observed systemic underestimation of μ is consistent with this in light of the expected inverse relationship between seeding and contamination described at the end of Section 5.1.

In Tables 1–3, for fixed n_I , $\alpha_{\hat{\theta}_{n_s, n_I}^{(\text{M2})}}$ always decreases for increasing n_s . This is reassuring, although not a necessity because it is possible that the synthetic dataset is atypical and more simulations (higher n_s) do not make it easier to approximate it.

For further analysis, we introduce two more symbols. One might consider a trivial estimator which assumes no contamination occurring: $\hat{\mu} = 0$, $\hat{\lambda}^\ell = n_s^{-1} n_I^{-1} \sum_{s=1}^{n_s} \sum_{i \in I} Y_i^{\ell, s}$. α_{triv} will denote the value of α for this trivial estimator. α_{θ_0} denotes a realisation of α with the true parameter θ_0 and n_s simulations.

n_s	n_{opt}	μ_{max}	θ_0	$\hat{\theta}_{n_s, n_I}^{(\text{M1})}$	$d^{(\text{M1})}$	$\hat{\theta}_{n_s, n_I}^{(\text{M2})}$	$d^{(\text{M2})}$	$\alpha_{\hat{\theta}_{n_s, n_I}^{(\text{M2})}}$
1	6	0.03	0.05	0.0480	4%	0.0460	8%	0.0056
			0.06	0.0575	4.17%	0.0573	4.5%	
			0.03	0.0298	0.67%	0.0311	3.67%	
			0.02	0.0239	19.5%	0.0225	12.5%	
6	3	0.03	0.05	0.0480	4%	0.0479	4.2%	0.0009
			0.06	0.0580	3.33%	0.0586	2.33%	
			0.03	0.0299	0.33%	0.0301	0.33%	
			0.02	0.0244	22%	0.0223	11.5%	

Table 3: Two estimates for a synthetic dataset with $n_I = 300 \times 300 = 90000$ vertices ($n_p = 268801$) and $\theta_0 = (0.05, 0.06, 0.03, 0.02)$.

n_s	n_{opt}	μ_{max}	θ_0	$\hat{\theta}_{n_s, n_I}^{(\text{M1})}$	$d^{(\text{M1})}$	$\hat{\theta}_{n_s, n_I}^{(\text{M2})}$	$d^{(\text{M2})}$	$\alpha_{\hat{\theta}_{n_s, n_I}^{(\text{M2})}}$
2	3	0.04	0.03	0.0295	1.67%	0.0293	2.33%	0.0011
			0.04	0.0402	0.5%	0.0401	0.25%	
			0.05	0.0522	4.4%	0.0520	4%	
			0.02	0.0192	4%	0.0195	2.5%	

Table 4: An estimate for a synthetic dataset with $n_I = 500 \times 500 = 250000$ vertices ($n_p = 748001$) and $\theta_0 = (0.03, 0.04, 0.05, 0.02)$.

Table 5 compares $\alpha_{\hat{\theta}_{n_s, n_I}^{(\text{M2})}}$, α_{triv} and α_{θ_0} for the four computer-generated datasets of Tables 1–4. Except for the smallest case, $n_I = 625$, α_{triv} is always greater than α_{θ_0} , as expected. Whereas α_{θ_0} decreases with increasing n_I , α_{triv} stays roughly constant. Importantly, $\alpha_{\hat{\theta}_{n_s, n_I}^{(\text{M2})}}$ also decreases broadly as n_I increases. Its value is much lower than α_{θ_0} but their ratio becomes ever less extreme as n_I grows. This is indicative of initially very strong, but later ever less pronounced overfitting.

Table 6 shows numerical evidence that $\alpha_{\theta_0} \rightarrow 0$ as $n_I \rightarrow \infty$, even with fixed n_s . For this, the four datasets studied in Tables 1–5 were extended with a fifth one with $n_I = 661 \times 661 = 436921$ ($n_p = 1308120$) and $\theta_0 = (0.02, 0.04, 0.05, 0.03)$. For this exercise, the common simulation count $n_s = 10$ was used.

The computations were conducted on a laptop computer equipped with a 2.5 GHz Intel Core i5-3210M processor and 8 GB RAM. The calculation of $\hat{\theta}_{n_s, n_I}^{(\text{M2})}$ for the data in Table 4 ($n_I = 250000$) took approximately 30 h.

n_I	n_p	n_s	n_{opt}	μ_{max}	$\alpha_{\hat{\theta}_{n_s, n_I}^{(\text{M2})}}$	α_{triv}	α_{θ_0}
625	1776	10	10	0.1	0.0126	0.6196	0.6783
625	1776	50	10	0.1	0.0107	0.5833	0.9022
625	1776	100	10	0.1	0.0062	0.5901	0.9006
10000	29601	20	10	0.05	0.0002	0.5841	0.0508
10000	29601	40	10	0.05	0.0001	0.5970	0.0461
90000	268801	1	6	0.03	0.0056	0.6317	0.0331
90000	268801	6	3	0.03	0.0009	0.6406	0.0099
250000	748001	2	3	0.04	0.0011	0.6443	0.0085

Table 5: A comparison of the values of the objective functions for the MSM estimator, the trivial estimator and the true value θ_0 . The four synthetic datasets used are the same as in Tables 1–4.

n_I	n_p	n_s	α_{θ_0}
625	1776	10	0.6783
10000	29601	10	0.0505
90000	268801	10	0.0115
250000	748001	10	0.0071
436921	1308120	10	0.0013

Table 6: Realisations of the objective function α for the true parameter value θ_0 for different synthetic dataset sizes.

6 Cross-contamination rate estimation for digital PCR in lab-on-a-chip microfluidic devices

Our motivation for investigating this problem is the need for quality control in parallelised biochemical experiments run in novel, lab-on-a-chip microfluidic devices for applications in basic research, biotechnology, medical diagnostics and rapid vaccine development. Our collaborators Dr Günter Roth and his group (Centre for Biological Systems Analysis [ZBSA], University of Freiburg) develop such microfluidic devices. The central element of their system is a rectangular well plate with 15 mm edge lengths, with more than 100,000 wells of 19 pℓ volume each. The wells on this chip are arranged in a hexagonal tiling pattern (honeycomb lattice).

Whereas the rival microfluidic technology uses an emulsion of water droplets flowing in an oil medium, this array-based setup fixes a spatial structure, allowing the otherwise neglected analysis of cross-contamination between reaction volumes. Our focus is on evaluating an experiment particularly well suited for this purpose, whose results generalise to other experiments conducted in this lab-on-a-chip device.

In the *digital PCR* experiment, a solution of DNA samples is injected onto the well plate, at such a low concentration that most wells receive 0 or 1 DNA molecule (hence the name *digital*). In the particular case, the solution is a mixture of three different DNA species. We call these template molecules *seeds*. The well plate is covered with a lid (a microscope slide) that is pre-coated with covalently bound DNA primers [15]. The well plate together with the lid serve to insulate the reaction volumes from each other. The DNA templates are amplified in each of the wells independently with a polymerase chain reaction (PCR). In more detail, the template molecules hybridise to the surface-bound primers and the PCR elongates these primers to form the complementary strand of the template. In the next heating step, the templates become resolved, whereas the generated complementary DNA strands stay covalently bound to the surface. The single-strand templates will bind to other surface-bound primers and turn them too into complementary strands via polymerisation. The result of the PCR cycles is that the whole glass surface above the well gets covered with immobilised complementary DNA strands. They mirror the spatial arrangement of the initial seed pattern of the wells.

After the PCR, the three complementary DNA species on the slide are identified via three specifically binding fluorescent hybridisation probes (fluorophores) and their presence or absence can be determined by imaging [16]. In the fluorescent image of the slide (Figure 2), we see either black background (where there was no seed), spots in one of the three primary colours indicating a single seed, and sometimes a mixture of two or three primary colours indicating heterogeneous seeding by multiple seeds. Sometimes we also see clusters of one colour, or an unusually high number of mixed colours, indicating cross-contamination between adjacent wells. This happens when the lid is not fitted tightly and during thermal cycling, liquid exchange occurs between reaction volumes around trapped air bubbles and dust particles. In the readout it remains unclear if two neighbours

with the same colour (or a single well with a mix of two colours, which has coloured neighbours) were initiated by two seeds or one contaminated the other (Fig. 2, bottom panel).

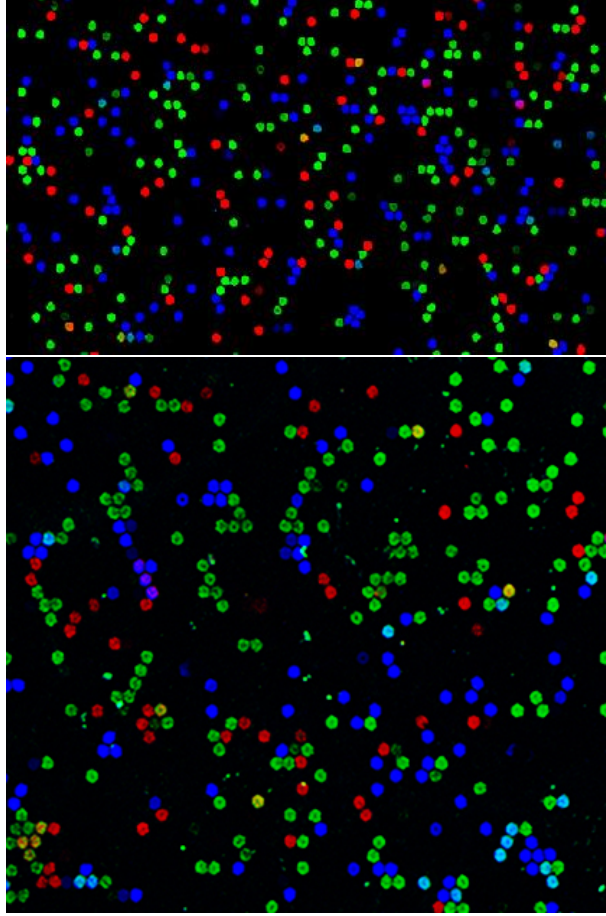


Figure 2: (*top*) Image of a glass slide from a digital PCR experiment with little sign of cross-contamination. [19] (*bottom*) Image of a slide with clustering fluorescent signals and a higher prevalence of cyan and yellow colours, suggesting higher cross-contamination rate.

For cross-contamination rate estimation for this experimental setup it is necessary to define a mathematical model of the physical process. It has to involve the triangular lattice, which is the dual of the hexagonal tiling, and colouring of its vertices. The total numbers of DNA templates of each type $\ell \in \{1, \dots, n_c\}$ present in the chip are likely well approximated by n_c discretised normal random variables. We can safely assume that each well receives a Poisson distributed random number of DNA templates of type ℓ because then due to the superposition property, the total number of type ℓ templates in the chip is also Poisson distributed, which is close to a normal distribution. The Bernoulli distributed (X_i^ℓ) used in our model for seeding are really just a proxy to the either zero or positive value of the corresponding Poisson distribution. From a value λ^ℓ of the Bernoulli parameter, we can infer the parameter $\tilde{\lambda}^\ell$ of the respective Poisson distribution through the identity $\lambda^\ell = 1 - e^{-\tilde{\lambda}^\ell}$.

It is also natural to model the possibility of contamination by open edges. It is a useful shortcut to draw the state of the edges independently of the seeding so that an open edge means only the possibility of propagation, which is contingent on the presence of seeds. There are modelling choices to be made. Contamination might be

- (i) unidirectional (there is the possibility of a pair of independent, oppositely oriented directed edges $\xi_{i \rightarrow j}$ and $\xi_{j \rightarrow i}$ between any two adjacent vertices $i \sim j$), or

(ii) symmetric (undirected edges ξ_{ij}).

Open edges might be best represented by

- (1) independent Bernoulli variables, or by
- (2) locally correlated 0–1 random variables.

Contamination might be

- (A) confined to neighbours, or
- (B) it might propagate via a series of open edges.

The choice of (ii,1,B) yields the model put forward in Section 1 (Figure 3). Its strength is that it can use standard percolation theory. Our MSM estimator was developed for this model.

For the quality certification of this lab-on-a-chip device, it is useful to estimate in addition to μ , the total number of vertices which belong to a non-trivial component of the percolation graph. These vertices are the wells which were not insulated from their neighbours. Beyond the digital PCR paradigm, in experimental setups where most wells are expected to give some signal, vertices that are connected to any other are likely to give false signals.

An easy upper bound results from noticing that each edge turns at most two additional vertices connected. For small values of μ , edges are actually unlikely to share endpoints. The number of edges is distributed according to a binomial distribution with parameters n_p and μ . Therefore the mean number of potentially contaminated vertices can be estimated as

$$\mathbb{E} \left[\sum_{|C| \geq 2} |C| \right] \leq 2\mu n_p \sim 6\mu n_I$$

where the asymptotic equality holds under the assumption that the boundary of I is ‘small’. For a concrete example, the conversion from n_p to n_I can be accurately determined.

Another approach results by noticing

$$\begin{aligned} \mathbb{E} \left[\sum_{|C| \geq 2} |C| \right] &= \mathbb{E} \left[n_I - \sum_{i \in I} \chi_{\{|C(i)|=1\}} \right] \\ &= n_I - n_I(1 - \mu)^6 + e \\ &= \left(6\mu - 15\mu^2 + \sum_{k=3}^6 \binom{6}{k} (-1)^{k+1} \mu^k \right) n_I + e, \end{aligned}$$

where e is the correction for boundary vertices.

Simpler cases are given by (i,1,A) and (ii,1,A) where the moments $\mathbb{E}[Y_i^\ell]$, $\mathbb{E}[Y_i^\ell Y_i^m]$ and $\mathbb{E}[Y_i^\ell Y_j^\ell]$ ($i \sim j$, $\ell \neq m$) can be computed explicitly. We used MATHEMATICA (Wolfram Research, Inc.) to deal with the many terms, and we report truncations of the complete result for space considerations in the case (i,1,A). It is anticipated in the practical application that $\mu < \lambda^\ell$ for every ℓ . For non-boundary vertices, under this assumption on the anticipated magnitudes, the dominant terms of

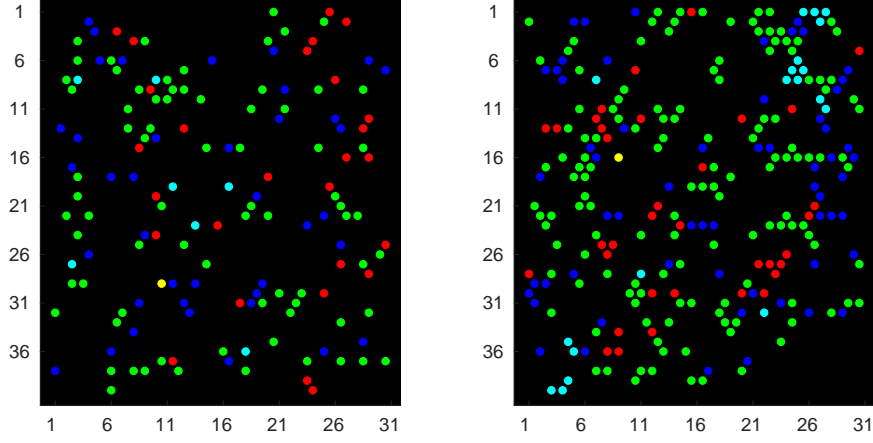


Figure 3: (*left*) Computer simulation of a glass slide from a digital PCR experiment under model (ii,1,B) with $\theta_0 = (\lambda^{\text{red}}, \lambda^{\text{green}}, \lambda^{\text{blue}}, \mu) = (0.02, 0.07, 0.05, 0.01)$ and relatively little sign of cross-contamination. (*right*) Computer-simulated slide with clustering fluorescent signals and a higher prevalence of cyan colour, suggesting higher cross-contamination rate. Here $\theta_0 = (0.02, 0.07, 0.05, 0.06)$.

the moments of interest in decreasing order are given as

$$\begin{aligned}
\mathbb{E}[Y_i^\ell] &= \mathbb{P}(X_i^\ell = 1) + \mathbb{P}(X_i^\ell = 0) \sum_{k=1}^6 \binom{6}{k} \mu^k (1-\mu)^{6-k} (1 - (1-\lambda^\ell)^k) \\
&= \lambda^\ell + 6\lambda^\ell \mu - 6(\lambda^\ell)^2 \mu - 15(\lambda^\ell)^2 \mu^2 + \mathcal{O}((\lambda^\ell)^5), \\
\mathbb{E}[Y_i^\ell Y_i^m] &= \mathbb{P}(X_i^\ell X_i^m = 1) + \mathbb{P}(X_i^\ell = 1, X_i^m = 0) \sum_{k=1}^6 \binom{6}{k} \mu^k (1-\mu)^{6-k} (1 - (1-\lambda^m)^k) \\
&\quad + \mathbb{P}(X_i^\ell = 0, X_i^m = 1) \sum_{k=1}^6 \binom{6}{k} \mu^k (1-\mu)^{6-k} (1 - (1-\lambda^\ell)^k) \\
&\quad + \mathbb{P}(X_i^\ell = X_i^m = 0) \sum_{k=1}^6 \binom{6}{k} \mu^k (1-\mu)^{6-k} (1 - (1-\lambda^\ell)^k) (1 - (1-\lambda^m)^k) \\
&= \lambda^\ell \lambda^m + 18\lambda^\ell \lambda^m \mu - 12((\lambda^\ell)^2 \lambda^m + \lambda^\ell (\lambda^m)^2) \mu + 30\lambda^\ell \lambda^m \mu^2 + \mathcal{O}(\max\{\lambda^\ell, \lambda^m\}^5).
\end{aligned}$$

For $\mathbb{E}[Y_i^\ell Y_j^\ell]$ ($i \sim j$), in the case $X_i^\ell + X_j^\ell = 1$, the empty vertex might have been contaminated by the seeded vertex, or it might have been contaminated from its five remaining neighbours. If $X_i^\ell = X_j^\ell = 0$, then one can separate cases according to the seeding status of the two shared neighbours of i and j . These considerations give

$$\mathbb{E}[Y_i^\ell Y_j^\ell] = (\lambda^\ell)^2 + 2\lambda^\ell \mu + 8(\lambda^\ell)^2 \mu + 2\lambda^\ell \mu^2 - 10(\lambda^\ell)^3 \mu + 9(\lambda^\ell)^2 \mu^2 + \mathcal{O}((\lambda^\ell)^5).$$

These $n_c^2/2 + 3n_c/2$ moment equations provide the opportunity to estimate the $n_c + 1$ parameters via the method of moments. Of these, it is $E[Y_i^\ell Y_j^\ell]$ where the first term with μ is highest up in the magnitude ranking, underpinning the physical intuition that the cooccurrence of a colour in two adjacent wells is the most informative moment about the contamination rate μ .

Notably, the model (ii,1,A) gives exactly the above moment equations if for any $(i, j) \in I_2$,

$$\begin{aligned} P(\xi_{i \rightarrow j} = 1) &= P(\xi_{j \rightarrow i} = 1) = \mu && \text{in model (i,1,A), and} \\ P(\xi_{ij} = 1) &= \mu && \text{in model (ii,1,A).} \end{aligned}$$

The reason is that the propagation of colours is limited to neighbours, so already second neighbours are ruled out. An edge between i and j makes a difference in any of the above three moments if and only if $X_i^\ell + X_j^\ell = 1$. Say, $X_j^\ell = 1 = 1 - X_i^\ell$. Then $\xi_{j \rightarrow i}$ has the same effect on these moments as ξ_{ij} , and also the same probability because one can marginalise over the state of $\xi_{i \rightarrow j}$. However, $E[Y_i^\ell Y_j^\ell Y_i^m Y_j^m]$ would differ between the models (i,1,A) and (ii,1,A). See also the Appendix of [10].

7 Discussion and open problems

This paper describes the solution of a statistical problem motivated by a concrete practical need. The mathematical modelling part is solved in one of multiple possible ways, and the choice of (ii,1,B) brings in bond percolation into the statistical model. The percolation is subcritical. The parameter estimation method we propose is the MSM, which gives a point estimate. We take steps towards proving that it is strongly consistent in the limit as the sample size n_I tends to infinity. It is an important point that the number of simulations per proposed parameter vector, n_s , can remain bounded to achieve this result.

What is unusual in our setting is that although the sample size is large, it is not independent (nor identically distributed). Introductory percolation theory is used to upper bound long-range dependencies between the n_I samples.

We have implemented the method and its accuracy is tested on synthetic datasets in practically relevant parameter ranges. Estimates for wetlab data are to be published by our collaborators Günter Roth and his co-workers in the microfluidics literature.

Parameter estimation in connection with a (static) percolation model is not common in the literature, apart from the quest for the critical value. Dynamic percolation models and dynamic random graphs on a fixed vertex set provide a framework for the contact network in modelling the spread of epidemics. Gilligan and Gibson have been particularly active in studying statistical problems for spatiotemporal models of plant epidemic spread [11, 17]. Gilligan and co-workers also conducted experiments with the fungal pathogen *Rhizoctonia solani* grown in a Petri dish to test how infection probability between a pair of lattice points (that is, the parameter μ of percolation in the directed case (i)) depends on their distance and how invasive spread (percolation) probability depends on nutrient availability in lattice points and on the distance between lattice points [2]. They also demonstrated that the random removal (blocking) of sites can hinder and even stop disease spread by driving it subcritical [18].

Beyond the almost sure convergence and the numerical studies with synthetic data, we cannot predict the accuracy of our estimator for instance in terms of confidence intervals. It is known that under regularity conditions, especially that the estimator is continuously differentiable with respect to the parameter θ , $\sqrt{n_I}(\hat{\theta}_{n_s, n_I} - \theta_0)$ is asymptotically normal with known limiting variance [12, Section 2.3.1]. It is also possible to choose Ω optimally, that is, to minimise this asymptotic variance [12, Section 2.3.4]. However, our estimator is not even continuous in θ because we use what is called a frequency simulator. It is unknown to us whether it is possible to replace the frequency simulator with some importance sampling to achieve asymptotic normality.

Maximum likelihood estimation (MLE) would have the advantage over MSM that its output is reproducible. Its computational cost might also be lower. Consider the following. We know that black areas have no seeds but we have no information about contamination (edges) in them. We also know that at boundaries between different colours, there is no open edge. Therefore, for a MLE, one needs to establish the probabilities of patches with a fixed colour without knowing which vertices were seeded and which got contaminated only.

We wonder if it is possible by using a generating function that encodes the probabilities of seeding and open edges to compute the total probability that the particular patch was created: each vertex in a patch has been seeded or contaminated from a seed somewhere within the patch. We were only able to derive this generating function for patches that are a linear chain of wells.

General finite, connected patch shapes (subgraphs) are called *(lattice) animals*. Bousquet-Mélou did much work on characterising them via generating functions [5, 6]. Our patches can arise as a disjoint union of adjacent connected components (animals). For our application, it would suffice to develop a recursion which allows one to compute generating functions of small patches (large patches are rare) with a computer algebra system. The difficulty is that the problem is two dimensional, and a patch must be split in all possible ways into two disjoint parts in the recursion. Any newly added vertex might have been seeded, or contaminated from the rest of the patch, but it might have itself contaminated other empty vertices of the patch.

Notably, the MSM estimator can be turned into an Approximate Bayesian computation (ABC) method very easily. One needs to fix a prior distribution on Θ and a small $\varepsilon > 0$. The ABC rejection algorithm draws finitely many independent $\theta \in \Theta$ parameter values from the prior distribution. The objective function (14) is evaluated for each proposed θ . The simulations used for the evaluation should no longer use common random numbers but independent ones, and n_s can be set to one. If the value of the objective function is less than ε , then the proposed θ is accepted, otherwise it is rejected. This way the set of accepted θ is a good approximation of the posterior distribution.

We have not yet tested model fit due to the lack of experimental data. As contamination is caused by the imperfect fit of the glass lid and trapped bubbles and dust, we anticipate that locally positively correlated open edges might be needed in the model. That is, case (ii,2,B) deserves close attention. One way of modelling positive correlations is to apply the Ising model to the edges. Let $\tilde{\xi}_{ij} = 2\xi_{ij} - 1 \in \{-1, +1\}$. Then the energy or the Hamiltonian function of a configuration ξ of open edges is

$$H(\xi) = -J \sum_{i < j < k} (\tilde{\xi}_{ij}\tilde{\xi}_{ik} + \tilde{\xi}_{ij}\tilde{\xi}_{jk} + \tilde{\xi}_{ik}\tilde{\xi}_{jk}) - \tilde{\mu} \sum_{(i,j) \in I_2} \tilde{\xi}_{ij}$$

for some $J > 0$ and $\tilde{\mu} > 0$, and in the first sum, out of the three terms those are missing where an adjacency condition is not met: $\tilde{\xi}_{ij} = 0$ if $i \not\sim j$, so that every pair of incident edges appear once. The probability of the system being in state ξ is proportional to $e^{-\beta H(\xi)}$ for some $\beta > 0$. Although we have two new parameters J and the inverse temperature β in addition to $\tilde{\mu}$, the increase in degrees of freedom is really just one, βJ and $\beta\tilde{\mu}$ relative to μ .

8 Acknowledgements

The authors are grateful to Günter Roth and Christin Rath (ZBSA, University of Freiburg) for proposing the problem, for their relentless help in clarifying details of the experimental protocol and for providing sample images. The authors also thank Robin Ryder (Paris Dauphine University) for suggesting the method of simulated moments and Ed Crane (University of Bristol) and Peter Pfaffelhuber (University of Freiburg) for insights. B. M. thanks the AXA Research Fund for their financial support in the form of a postdoctoral fellowship, and the Isaac Newton Institute for Mathematical Sciences (Cambridge, UK) for support and hospitality during the programme *Stochastic*

dynamical systems in biology: numerical methods and applications when work on this paper was undertaken. This work was thereby supported by EPSRC Grant Number EP/K032208/1.

References

- [1] Michael Aizenman and Charles M. Newman. Tree graph inequalities and critical behavior in percolation models. *Journal of Statistical Physics*, 36(1–2):107–143, 1984. doi: 10.1007/BF01015729.
- [2] Douglas J. Bailey, Wilfred Otten, and Christopher A. Gilligan. Saprotrophic invasion by the soil-borne fungal plant pathogen *Rhizoctonia solani* and percolation thresholds. *New Phytologist*, 146(3):535–544, June 2000. ISSN 1469-8137. doi: 10.1046/j.1469-8137.2000.00660.x. URL <http://dx.doi.org/10.1046/j.1469-8137.2000.00660.x>.
- [3] Felix Beck. Parameter estimation in a percolation model with coloring. Master’s thesis, Institute for Mathematics, University of Freiburg, Germany, 2015.
- [4] J. van den Berg and H. Kesten. Inequalities with applications to percolation and reliability. *Journal of Applied Probability*, 22(3):556–569, Sep 1985. ISSN 00219002. doi: 10.2307/3213860. URL <http://www.jstor.org/stable/3213860>.
- [5] Mireille Bousquet-Mélou. New enumerative results on two-dimensional directed animals. *Discrete Mathematics*, 180:73–106, 1998. doi: 10.1016/S0012-365X(97)00109-X.
- [6] Mireille Bousquet-Mélou and Andrew Rechnitzer. Lattice animals and heaps of dimers. *Discrete Mathematics*, 258:235–274, 2002. doi: 10.1016/S0012-365X(02)00352-7.
- [7] John D’Errico. `fminsearchbnd`, `fminsearchcon` MATLAB files, 2012. URL <http://uk.mathworks.com/matlabcentral/fileexchange/8277-fminsearchbnd--fminsearchcon>.
- [8] Nasrollah Etemadi. On the laws of large numbers for nonnegative random variables. *Journal of Multivariate Analysis*, 13(1):187–193, 1983. ISSN 0047-259X. doi: 10.1016/0047-259X(83)90013-1. URL <http://www.sciencedirect.com/science/article/pii/0047259X83900131>.
- [9] C. M. Fortuin, P. W. Kasteleyn, and J. Ginibre. Correlation inequalities on some partially ordered sets. *Communications in Mathematical Physics*, 22(2):89–103, 1971. ISSN 0010-3616. doi: 10.1007/BF01651330.
- [10] H. L. Frisch and J. M. Hammersley. Percolation processes and related topics. *Journal of the Society for Industrial and Applied Mathematics*, 11(4):894–918, 1963. ISSN 03684245. URL <http://www.jstor.org/stable/2946482>.
- [11] G. J. Gibson, W. Otten, J. A. N. Filipe, A. Cook, G. Marion, and C. A. Gilligan. Bayesian estimation for percolation models of disease spread in plant populations. *Statistics and Computing*, 16(4):391–402, 2006. ISSN 1573-1375. doi: 10.1007/s11222-006-0019-z. URL <http://dx.doi.org/10.1007/s11222-006-0019-z>.
- [12] Christian Gouriéroux and Alain Monfort. *Simulation-based econometric methods*. Oxford University Press, Oxford, UK, 2002.
- [13] Christian Gouriéroux and Alain Monfort. Simulation based inference in models with heterogeneity. *Annales d’Économie et de Statistique*, 20–21:69–107, 1991. ISSN 0769489X. URL <http://www.jstor.org/stable/20075807>.

- [14] Geoffrey Grimmett. *Percolation*. Grundlehren der mathematischen Wissenschaften. Springer Berlin Heidelberg, 1999.
- [15] Jochen Hoffmann, Sebastian Hin, Felix von Stetten, Roland Zengerle, and Günter Roth. Universal protocol for grafting PCR primers onto various lab-on-a-chip substrates for solid-phase PCR. *RSC Advances*, 2:3885–3889, 2012. doi: 10.1039/c2ra01250b.
- [16] Jochen Hoffmann, Martin Trotter, Felix von Stetten, Roland Zengerle, and Günter Roth. Solid-phase PCR in a picowell array for immobilizing and arraying 100 000 PCR products to a microscope slide. *Lab on a Chip*, 12:3049–3054, 2012. doi: 10.1039/c2lc40534b.
- [17] Jonathan J. Ludlam, Gavin J. Gibson, Wilfred Otten, and Christopher A. Gilligan. Applications of percolation theory to fungal spread with synergy. *Journal of The Royal Society Interface*, 9(70):949–956, 2012. ISSN 1742-5689. doi: 10.1098/rsif.2011.0506. URL <http://rsif.royalsocietypublishing.org/content/9/70/949>.
- [18] Wilfred Otten, Douglas J. Bailey, and Christopher A. Gilligan. Empirical evidence of spatial thresholds to control invasion of fungal parasites and saprotrophs. *New Phytologist*, 163(1): 125–132, July 2004. ISSN 1469-8137. doi: 10.1111/j.1469-8137.2004.01086.x. URL <http://dx.doi.org/10.1111/j.1469-8137.2004.01086.x>.
- [19] Christin Rath. DNA-Kopierprozess mit Thrombin-Aptamer Mikroarrays (in German). Master’s thesis, Centre for Biological Systems Analysis (ZBSA), Faculty of Biology, University of Freiburg, Germany, 2014.
- [20] M. F. Sykes and J. W. Essam. Exact critical percolation probabilities for site and bond problems in two dimensions. *Journal of Mathematical Physics*, 5(8):1117–1127, 1964. doi: <http://dx.doi.org/10.1063/1.1704215>. URL <http://scitation.aip.org/content/aip/journal/jmp/5/8/10.1063/1.1704215>.